UNIVERSITY OF CINCINNATI

Date: 10 - 20 - 2006

I, Srikant Srinivasan **,**

hereby submit this work as part of the requirements for the degree of:

Master of Science

in:

Electrical Engineering

It is entitled:

A Compact Model for the Coaxially Gated Schottky Barrier Carbon Nanotube Field Effect Transistor

This work and its defense approved by:

Chair: Dr. Harold W. Carter

Dr. Marc M. Cahay

Dr. Carla Purdy

A Compact Model for the Coaxially Gated Schottky Barrier Carbon Nanotube Field Effect Transistor

A thesis submitted to the
Division of Research and Advanced Studies
of the University of Cincinnati
in partial fulfillment of the requirement for the degree of

Master of Science

in the Department of
Electrical and Computer Engineering and Computer Science
of the College of Engineering

2006

By

Srikant Srinivasan

B.Tech., Jawaharlal Nehru Technological University,
India, 2003

Committee Chair: Dr. Harold W. Carter

Abstract

Carbon nanotubes have generated much interest in the last few years for application in electronic devices because of their demonstrated ability to serve as a possible alternative to silicon technology for fabrication of nanoscale electronic devices, in view of the challenges faced by the continuous scaling of existing silicon technology. Much effort has been applied into the understanding of the underlying principles and the device physics of carbon nanotubes as also in the fabrication of suitable devices with various geometries. The current simulation approaches used for generating reliable device characteristics for these devices can be highly complex and are most often computationally intensive. There is , therefore, a need to develop alternative approaches that are simple and computationally less intensive and yet adequately accurate, especially in the context of design and evaluation of circuits using these devices.

In this thesis, we have performed a detailed study of the working principles of semiconducting carbon nanotubes with the objective of developing compact models that can replicate, with good accuracy, the current-voltage characteristics of these devices. Specifically, compact models have been developed for the current - voltage characteristics for the cylindrical gate Schottky-Barrier Carbon Nanotube Field Effect Transistor (SB-CNFET), consistent with experimental results published in the literature. These models reflect the dependence of the transistor characteristics on various physical parameters such as different dielectrics and different gate insulator thicknesses. These compact models can be readily integrated into any of the existing Hardware Description Languages for building and evaluating circuits based on SB-CNFET or hybrid CMOS/ CNFET technology.

Acknowledgements

I am greatly indebted to my Master's thesis advisor, Dr. Hal Carter, for his perpetual encouragement and guidance – both academic and non-academic – during the course of this thesis work. It was a wonderful experience working with him and I stand to have gained much through my interactions with him. I am now able to view every problem in the 'system' perspective.

I would also like to express my deep gratitude for Dr. Marc Cahay for patiently translating the complex world of device physics into more reasonably understandable terms. He is one of most approachable persons I have met and I often found myself ending up at his office on the occasions that I got stuck in the theory of nanotubes.

The valuable discussions with Dr. Supriyo Datta on nanoscale devices have helped much in strengthening basic concepts in this field. I would also like to thank my colleagues at Purdue University – thanks Jagadeesh – for helping out me with a crash course on Latex and getting this thesis written. It is also my pleasure to thank Dr. Carla Purdy for readily agreeing to serve on my thesis committee on short notice.

The constant support and encouragement of my parents and siblings cannot be adequately acknowledged. Any attempt to express my gratitude for them will only fall short of the mark.

To Appa and Amma,

for your support all the way.

Contents

List of Figures

Chapter 1

Introduction

1.1 Recent trends in Carbon Nanotube Electronics

Carbon nanotubes (CNTs) have been extensively studied for use in a variety of electronic and non-electronic applications since they were first discovered by Iijima[1] in 1991. CNTs can be either metallic or semiconducting in nature. In the last several years, the use of single walled semiconducting CNTs as the channel in Field Effect Transistors has been actively investigated while metallic CNTs have received the same consideration for use as interconnects in Integrated Circuits. Given their ability to serve as a potential alternative to existing Silicon CMOS technology[2] and overcome the hurdle of the scaling limits of Silicon technology, CNTs have been a subject of rigorous theoretical analysis. Extensive work has been done in trying to establish fabrication techniques to reliably reproduce these devices for large scale production. However, the challenges faced in fabricating single-walled CNTs

have been formidable.

Briefly, some of the popular techniques used for growth of CNTs currently[3] are

- Pulsed laser vaporization of graphite in the presence of an inert gas and metal catalysts. The carbon vapors condense into single walled nanotubes. This method does not lend itself to large scale production.
- Electric Arc Discharge of an anode containing metal catalysts that react with Carbon vapors to form single walled tubes. This method is more rapid than the the earlier one but controlled growth of nanotubes to obtain only the single walled kind is still not at a mature stage.
- Plasma Enhanced Chemical Vapor Deposition, High Pressure Carbon Monoxide conversion. These techniques too are yet to prove the ability for reliable large scale production of single walled CNTs

The current state of the art for fabricating CNFETs uses one of the above techniques for growing CNTs on a substrate. Then a suitable method like Atomic Force Microscopy is used to determine the location of CNTs and a metal, such as gold, is deposited on either end to make contacts. A prototype transistor of this variety fabricated at an IBM facility is shown in Fig. 1.1. This is a popular CNFET configuration at this time, due to the feasibility of fabrication. It is referred to as the planar CNFET[4], since either a topside or backside planar gate is used to control the semiconducting nanotube. Metal

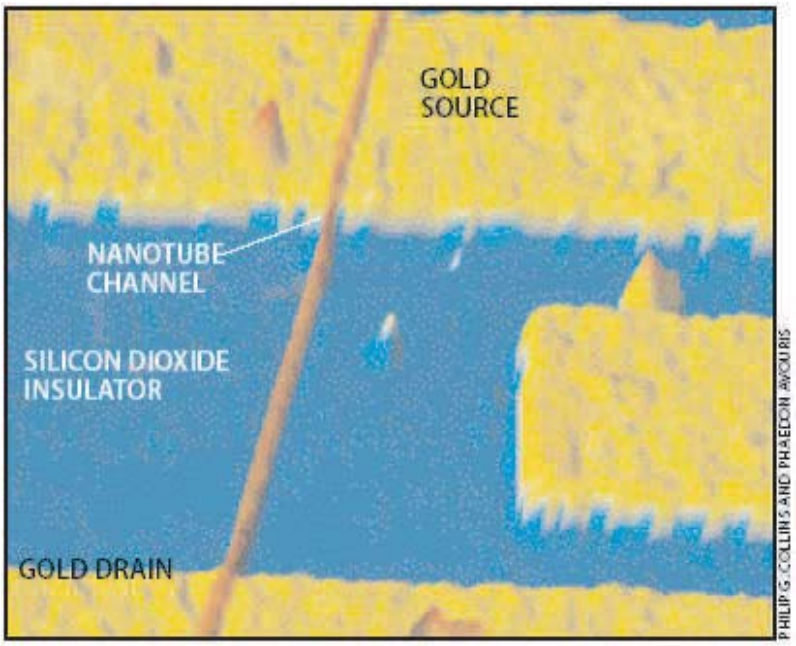

Figure 1.1: A planar CNFET fabricated at IBM

contacts deposited on either end of the nanotube form rectifying Schottky barriers.

While there has been speculation[5] about growing ropes of metallic nanotubes interspersed with semiconducting nanotubes to form naturally occurring devices, this occurrence has been rarely observed. Another configuration that has been investigated – shown in Fig. 1.2 – is the side gate variety, wherein a nanotube is grown vertically on a substrate and the gate lies beyond the source or drain. However, theoretical simulation[6] of such geometry shows insufficient gate control as compared to the planar geometry.

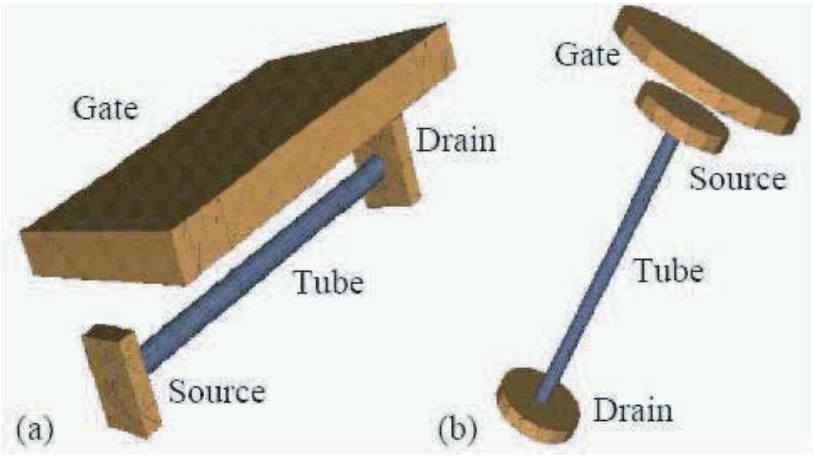

Figure 1.2: (a)Lateral and (b)Axial gated CNFET geometry

1.2 Related work - Modeling and Simulation

From a theoretical perspective, analysis of CNTs can get highly involved. In fact the current work on Carbon Nanotube FETs often involves computationally intensive numerical procedures such as Monte Carlo analysis and, more often than not, requires efficient algorithms for numerically solving Green's function[7] for the Hamiltonian matrix obtained by applying Schroedinger's equation. A typical CNFET simulation through a solution of Greens Function can run into several hours. A simulation of an Integrated Circuit containing several thousands of CNFETS is therefore not feasible even with the use of a grid of parallel computers. This disadvantage of accurate atomistic simulation approaches to CNFETs greatly stresses the need for the development of compact models that can run much faster even if they suffer from a slight reduction in accuracy. These models are usually some form of self consistent solutions of Poisson equation or a Schroedinger-Poisson solver[12, 13]. Also, there is much scope for integration of these compact models into standard Hardware Description Languages such as VHDL, VHDL-AMS, Verilog - to name a few - so that circuits and systems composed entirely of CNTs or hybrid CNT/ Si CMOS can be modeled and the behavior of these systems and their applicability can be gauged. However, there is yet work to be done in developing CNFET models for use by HDLs.

1.3 Problem Statement and Scope

In this thesis, a detailed study of the theory of Carbon Nanotubes was undertaken through numerical simulation to derive compact models for one popular geometry of the CNFET, namely the Schottky-Barrier CNFET (SB-CNFET). These models have been generated for incorporation in the model library of any standard Hardware Description Language. The approach used was self consistent solutions to the Poisson equation for the potential profile generated by a coaxial cylindrical gate. Some of the variables that were tweaked were the gate dielectric thickness, gate dielectric constant and source/drain contact metal work functions. This model relies on the tunneling mechanism at the source/ drain Schottky contacts for current flow. In addition, thermionic current components too have been included to determine the overall picture. This will be discussed in detail in subsequent chapters.

1.4 Outline of Thesis

Having introduced the readers to a brief history of Carbon nanotube Electronics and the development in this area in the last few years, the subsequent chapters of this thesis are organized as follows:

- Chapter 2 presents the underlying physics and electronic structure of the CNT in detail. In particular, an expression for the nanotube density

of states is derived. A comparison is then made between nanotubes and conventional silicon technology for application to integrated circuits.

- Chapter 3 delves into the electrostatics of the Schottky Barrier CNFET and the equations for charge and current as a function of the applied voltage are derived and examined. These equations culminate in the development of a compact model for the SB-CNFET and the dependance of the transistor characteristics on other parameters such as the gate insulator, physical dimensions etc are studied and incorporated into the model.

- Chapter 4 gives the simulated results of the compact model developed in Chapter 3. The compact model was coded as Matlab scripts and the results of the simulation of this model in Matlab are incorporated into Chapter 4 with a brief explanation for each of these results.

- Chapter 5 concludes the work undertaken in this thesis and looks at the scope for improvement of compact modeling by other approaches.

This thesis work is one of the first attempts to integrate nanoscale device modeling into the traditional circuits and systems modeling at the Distributed Processing Lab at University of Cincinnati. As such, the results have been presented with a view of providing the foundation for the basic understanding of nanoscale devices for my colleagues at University of Cincinnati, new to this regime of device scale.

Chapter 2

The Carbon Nanotube – Electronic Structure and Properties

In this chapter, we briefly review the physics involved in modeling Carbon nanotubes and look at some of the unique properties that make CNTs a very good substitute for a Silicon MOSFET. This is followed by a qualitative analysis of the behavior of a CNFET and we see that its working is quite similar to that of a conventional Si MOSFET. We then present some devices which have been fabricated and show how the transistor characteristics of these devices make a very strong case for the use of CNTs in FETs.

2.1 Overview of the Nanotube Electronic Structure

The physical structure of a carbon nanotube is easily understood when it is viewed as a two dimensional monatomic layer of graphene that has been rolled up to form a hollow cylinder. The carbon atoms in graphene are ordered in a hexagonal 'honeycomb' lattice arrangement as shown in Fig.2.1. The electrical properties of the CNT are determined by the manner in which this sheet of graphene is rolled up. The circumference of the nanotube – i.e, the rolled up graphene sheet – is expressed in terms of a 'chirality' vector **C** that maps two equivalent sites in the 2-D graphene sheet. The chirality vector can be expressed as **C**= n**a1** + m**a2** where **a1** and **a2** are the unit vectors of the 2-D graphene lattice. It is standard practice in literature to express nanotubes in terms of the integers (n,m). The ability of the nanotube to behave either as a semiconductor or a metal is governed by the behavior of the lowest energy sub-band, which can be derived by evaluating the basis vectors in the first Brillouin zone.The two possible configurations of carbon nanotubes are

- $n = m$: This is referred to as the 'armchair' configuration as shown in Fig.2.1 [26]. The nanotubes formed in this configuration are always metallic in nature. This is because the energy surfaces describing the conduction band and valence band touch each other at the $'\Pi'$ points

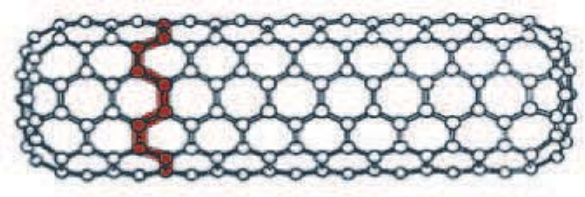

Figure 2.1: SWNT in the armchair configuration

when evaluated in the E-K space. Thus the nanotube behaves as a 'zero gap' semiconductor in this configuration.

- $n \neq m$: This is referred to as the 'zig-zag' configuration – shown in Fig.2.2. CNTs in this configuration can be either metallic or semiconducting in nature depending on whether n-m is a multiple of 3. CNTs in which n - m $\neq$ 3 behave as quasi-metallic nanotubes with band gaps that vary inversely with the square of nanotube radius[22]. Readers interested in this topic are referred to the paper by Mintmire and White[22] for a more detailed analysis of the CNT structure in E-K space. However, for practical purposes, roughly a third of the zig-zag nanotubes are metallic, while the rest are semiconducting.

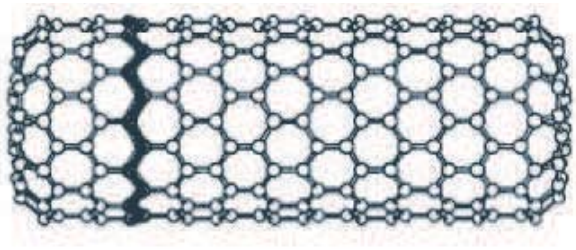

Figure 2.2: SWNT in the Zigzag configuration

2.1.1 A qualitative analysis of the Nanotube Density of States

In a graphene sheet, each unit cell can be expressed in terms of the two basis vectors **a1** and **a2** in real space as shown earlier. These vectors can be expressed in the cartesian co-ordinate system as:

$$\mathbf{a1} = a_0(\frac{\sqrt{3}}{2}\mathbf{x} + \frac{1}{2}\mathbf{y}) \tag{2.1}$$

$$\mathbf{a2} = a_0(\frac{\sqrt{3}}{2}\mathbf{x} - \frac{1}{2}\mathbf{y}) \tag{2.2}$$

where $a_0 = \sqrt{3}\mathrm{a}_{cc}$ and a_{cc} is the nearest neighbor atomic distance in graphene and has a value of 1.42 Angstrom.

This gives the basis vectors **b1** and **b2** in the reciprocal lattice space as the following:

$$\mathbf{b1} = b_0(\frac{1}{2}\mathbf{x} + \frac{\sqrt{3}}{2}\mathbf{y}) \tag{2.3}$$

$$\mathbf{b2} = b_0(\frac{1}{2}\mathbf{x} - \frac{\sqrt{3}}{2}\mathbf{y}) \tag{2.4}$$

where $b_0 = \frac{4\Pi}{\sqrt{3}a_0}$. The "dispersion relation" is then obtained for the carbon nanotube by applying the periodic boundary condition

$$\mathbf{k} \cdot \mathbf{c} = 2\Pi \tag{2.5}$$

where $\mathbf{c}$ is the circumferential vector and $\mathbf{k}$ is the allowed wave vector obtained from the basis vectors in the reciprocal space. The dispersion relation gives us the Energy dependance on the wave vector $\mathbf{k}$ and the Density of States (DOS) can be computed from this dispersion relation. The details of this procedure are clearly explained in the book by Datta[24].

The 1-D nanotube DOS computed[5] for the lowest sub-band of a Single Walled Nanotube can then be expressed as:

$$D(E) = \frac{4}{\Pi\hbar v_f} \frac{|E|\Theta(|E| - \Delta)}{\sqrt{E^2 - \Delta^2}} \tag{2.6}$$

where the Fermi velocity $\mathrm{v}_f = 8.1x10^5$ m/s and the energy gap is given by

$$2\Delta = \frac{2\hbar v_f}{3R} \tag{2.7}$$

where R = radius of the nanotube and Θ(x) is the Heaviside Unit step function. This basically tells us that the nanotube DOS for the electrons begins upwards from the conduction band edge and that of the holes begins downward from the valence band edge. Also it is shown in [25] that the Fermi level of the nanotube lies in the middle of the bandgap. Therefore, the Density

of States has a symmetric distribution on either side of the Fermi level and the conduction and valence bands are symmetric, which is advantageous for complementary operations.

2.1.2 A note on Multi-Walled Nanotubes

CNTs can be single-walled (composed of a single rolled up sheet of graphene) or multi-walled (several concentric cylinders of graphene). Single Walled nantubes (SWNTs) usually have a diameter of 1-2 nm and can go upto several microns in length. The electronic structure and properties of Multi-Walled nanotubes (MWNT) have been found to be governed by the outermost wall[4]. Therefore, the bandgap dependance on the radius of the outermost wall causes MWNTs to be usually metallic in nature. Also bundles of MWNTs are easily grown as long ropes , hence, these nanotubes have shown much promise as a substitute for interconnects in CMOS technology. This thesis work will, however, be limited to the study and application of single wall nanotubes as semiconducting channels in devices.

2.2 Carbon Nanotubes Vs Silicon

As mentioned earlier, the length of SWNTs are far greater than their circumferential dimensions. They can, therefore, be considered as one-dimensional (1-D) structures. Also, since nanotubes are rolled up sheets of graphite, the

atoms on either edge of the graphene sheet bond with each other thus leaving no unsatisfied dangling bonds. The electronic structure of SWNTs can, therefore, be determined by the application of periodic boundary conditions. These properties translate into some important advantages over Silicon.

- CNTs enjoy one-dimensional carrier transport. The charge travelling through the devices experiences very little phase scattering compared to silicon and the transport is often ballistic. The resistance of these devices approaches the quantum limit. The two terminal conductance is given by the Landauer equation

  $$G = (2e^2/h)*\sum T_i$$

  where T_i is the transmission coefficient of the i^{th} contributing sub-band. For SWNT we usually consider the lowest sub-band since the higher sub-bands lie beyond the electrochemical potentials of the source/ drain.

- Silicon often has dangling bonds near the surface and has to be chemically passivated by the growth of Silicon-dioxide. However, a major contribution to scattering in Silicon FETs occurs at the surface of the Si/ SiO_2 interface. CNTs, on the other hand, do not have such dangling bonds and therefore the carriers along the surface do not experience as much scattering or influence of interface traps.

- The self - passivated surface of CNTs implies that these devices can utilize a variety of high κ dielectrics and are not limited to the use of

silicon dioxide. Therefore, the gate has better control over the charge carriers in the channel than Si MOSFETs. Also, Fermi-level pinning at the metal-nanotube interface is weak, wherefore it is possible to utilize a variety of contact metals – resulting in different Schottky barrier heights – to obtain the desired transistor characteristics.

- There is strong covalent bonding between Carbon atoms in a nanotube thus giving them very high mechanical and thermal stability. The possibility of realizing current densities as high as $10^9 \mathrm{A/cm}^2$ has been predicted[8].

- The presence of the Fermi level in the middle of the bandgap of an intrinsic nanotube also means that the electrons and holes have the same effective mass. This is advantageous for complementary operations in Integrated Circuits.

Chapter 3

Modeling the Coaxially–gated Schottky-Barrier CNFET

In the previous chapter, we briefly reviewed the electronic structure of the Carbon nanotube and the advantages to be gained by implementing it as the channel of a FET. While most CNFETs in use are of the planar geometry, it is quite obvious that optimum transistor control can be achieved when the channel is encapsulated within a coaxial gate. In this chapter, we lend our focus to the working principles of the Schottky Barrier CNFET that uses a coaxial gate and develop a compact model to simulate its response. The SWNT, which forms the channel, can be used either in the extrinsic form or can simply be left undoped. The source and drain end of the nanotube terminate in metal contacts which are rectifying in nature.

Looking back at the typical Silicon MOSFET, we see that the contacts are ohmic in nature and are deposited in areas of highly doped source and drain regions. The MOSFET is so designed that the carriers flowing into the channel typically encounter minimum resistance at the contacts and the flow of current through the device is controlled by the applied gate voltage. In a nanotube, however, the carriers experience almost ballistic transport. The presence of Schottky barriers indicates that the transistor can be so designed, that the flow of current through the device is dictated to a great extent by the metal contact properties. The different possible methods of engineering the CNFET will be examined in the next section.

3.1 Electrostatics of the SB-CNFET

For the coaxially gated SB-CNFET – we shall henceforth refer to it simply as the SB-CNFET – shown in Fig.3.1, we see that the gate dielectric spans over the entire length of the nanotube and that this device has metal contacts that greatly exceed the dimensions of the nanotube itself.

The nanotube has a radius R_t and is surrounded by a cylinderical gate of radius R_g. Typically the value of R_t varies anywhere between 0.6 – 2 nm while the length of the nanotube L_t varies from 50nm to several microns. The gate dielectrics typically used for CNFETS are Silica, Alumina or Zirconia. Like a MOSFET, the electrostatics of the SB-CNFET can depend to a great

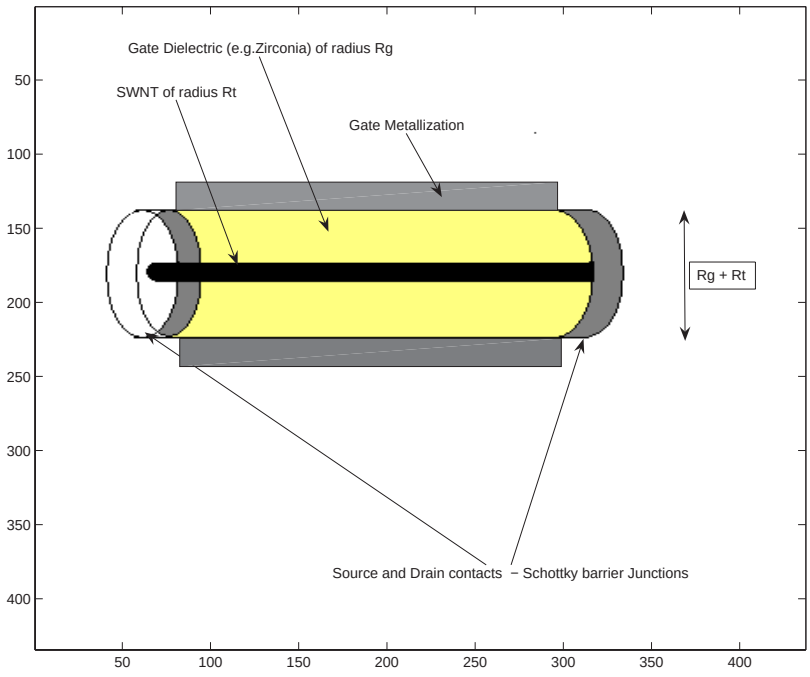

Figure 3.1: Construction of a coaxially-gated SB-CNFET

extent on its physical structure such as the dimensions of gate radius, the extent of the channel (nanotube) encapsulated within the dielectric and the thickness of the metal contacts and the work functions of the source, drain and gate metals.

The presence of 'bulk' metal contacts, as shown in Fig.3.2, causes the potential profile of the source and drain to be governed by the work functions of the metal contacts and the voltage applied on the contacts and the gate does not have much control over the nanotube in these regions. This is

because the field due to the image charges on the source and drain contacts extends into the tube. The distance over which the presence of this field is felt can be approximated to be equal to the dimensions of the gate radius R_g. Beyond this distance from the contacts, the effect of the gate voltage is felt more strongly on the channel. Again, the local electrostatics at the ends will depend on whether the gate extends all the way to the ends of the tube. The electrostatics of partially gated CNFETs has been studied in [14].

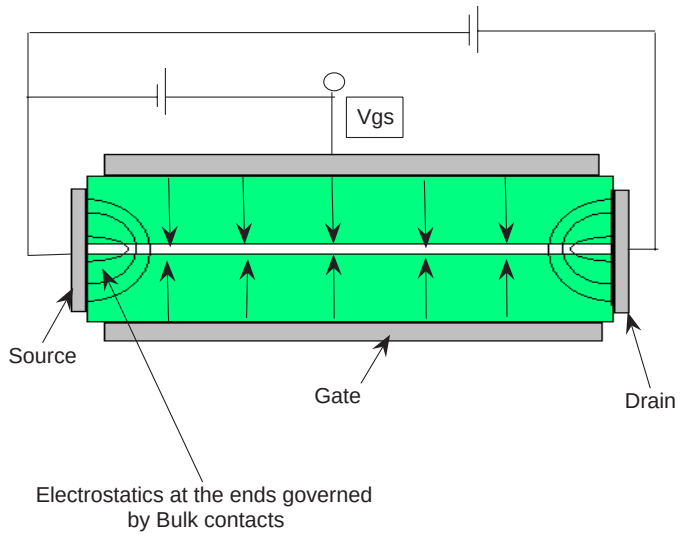

Figure 3.2: Electrostatics of the coaxially-gated SB-CNFET

If the source/ drain contacts are of the same dimensions as the tube radius R_t, then the effect of the gate is felt strongly even at the contacts and the gate

voltage can modify the Schottky barrier characteristics at the contacts. For the case of bulk contacts, however, there is charge transfer onto the nanotube depending on the difference in work functions and this governs the barrier profile. The source/ drain metals of the SB-CNFET being modeled in this thesis are assumed to have the same workfunction as the intrinsic nanotube for the sake of convenience. The band profile for such a device in thermal equilibrium is shown in Fig. 3.3.

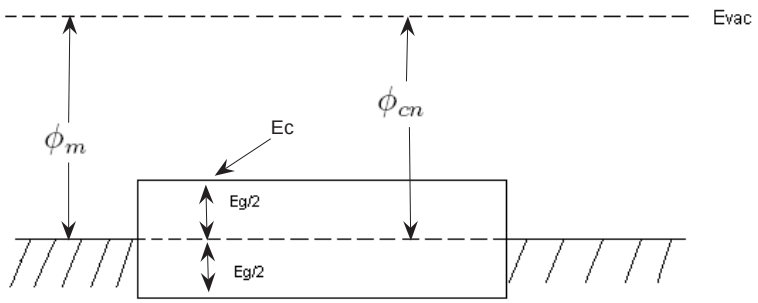

Figure 3.3: Equilibrium band profile

We can see that the intrinsic Fermi level of the nanotube is aligned with the work function of the metal. Also, it may be recalled that the Fermi level

lies right in the middle of the bandgap of the nanotube. The value of the bandgap in eV of this tube is given by

$$2\Delta = \frac{2\hbar v_f}{3R_t} \tag{3.1}$$

where R_t = radius of the nanotube in nm, $v_f = 8.1x10^5$ m/s, is the Fermi velocity of carriers in the nanotube.

3.2 Nanotube Charge Density

In equilibrium, the net charge density on the nanotube is zero because of the symmetric band profile. When a positive gate voltage is applied to nanotube, the conduction band moves down and the Fermi level moves closer to the conduction band. Consequently charge is induced in the conduction band. The source/ drain regions are, however, held by the metal work functions and consequently a Schottky barrier is formed at the ends. This is shown in Fig.3.4

3.2.1 A self-consistent solution for charge density

It can be seen that in low dimensional semiconductors where energy levels tend to be more discretized, – unlike bulk semiconductors, which have a

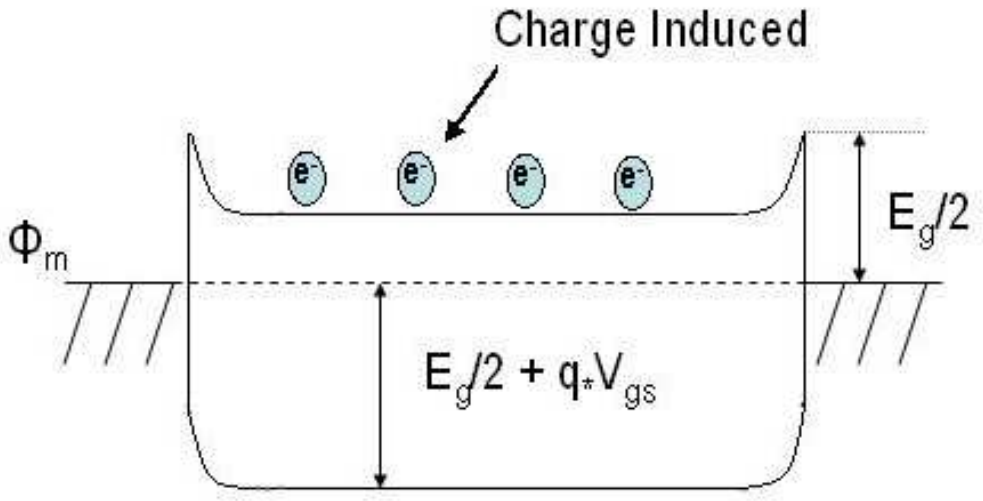

Figure 3.4: Band profile under Applied gate voltage

parabolic density of states vs. energy– the addition of charge to the semiconductor causes the available states to float up in the energy scale. This means that the addition of further charge will require a lot more applied potential, as more and more states get filled up. A similar argument can be applied while computing the charge density of carbon nanotubes. In this case, a simple capacitance expression is used to calculate the change in the band profile due to the accumulation of charge on the tube. The charge density – which is obtained from the band profile in the first place – is then recomputed taking into account the modification in the band profile and again the new band profile is computed taking into account this charge density and so forth. Thus the band profile of the nanotube and charge density have to be

repeatedly solved in this iterative manner until they eventually attain values that are consistent with each other.

The Fermi-Dirac probability for the occupation of an energy state 'E' is given by

$$f(E) = \frac{1}{1 - \exp \frac{(E-Ef)}{K_B T}} \tag{3.2}$$

where K_B is the Boltzmann constant. At room temperature, i.e. T = 300 Kelvin, $K_B T \simeq 25.6$ meV

The general expression for calculating the charge density is

$$n = \int_{-\infty}^{+\infty} f(E) D(E) dE \tag{3.3}$$

If η is the mid-length charge density on a nanotube channel, then the dependance of the local potential on this charge is given in terms of the gate capacitance as:

$$U = \frac{e^2 \eta}{C_{ins}} \tag{3.4}$$

where C_{ins} is the gate capacitance per unit area given by

$$C_{ins} = \frac{\varepsilon_{ins}}{t_{ins}} \tag{3.5}$$

This local potential 'U' causes the nanotube DOS to float up and must be taken into account for computing the charge density.

Using the expression for the nanotube Density of States D(E), given in

2.6, and taking into account the effect of the local potential from 3.4, we can compute the mid-length charge density from 3.3 as

$$\eta = \int_{Ec}^{+\infty} D(E + Vgs - U) \cdot f(E) dE \tag{3.6}$$

Equations 3.4 and 3.6 are solved self-consistently using Newton-Ralphson method to obtain the charge density for an applied gate voltage Vgs. It can also be seen that, for a negative voltage applied at the gate, the same expression holds for computing the hole charge density and the band profile obtained will simply be a mirror image of that observed in Fig.3.4

Quantum Capacitance

In deriving the self consistent charge density on the nanotube, we made use of a simple capacitance relation involving the charge on the nanotube and the gate dielectric capacitance. However, there is an additional capacitance term, namely, the quantum capacitance [9] of the nanotube. This term is proportional to the nanotube DOS and is given by

$$C_q = q^2 \cdot \bar{D} \tag{3.7}$$

This capacitance appears in series with the nanotube gate capacitance. However, since the magnitude of the quantum capacitance of the nanotube is far greater than the gate capacitance, we can approximate the overall capaci-

tance as shown in 3.5

Triangular Barrier Approximation

An approximation for computing the band profile towards either end of the nanotube is made as follows: Over a distance R_g from the source/drain end, the electrostatic potential is a linear combination of applied gate voltage and the source voltage (ground, in our case). Therefore, we have a triangular barrier profile at the Schottky contacts. The width of the base of this triangular barrier is R_g and the height is given by:

$$h = \phi_m - \phi_{cn} + \frac{Eg}{2} \tag{3.8}$$

3.3 Determining the SB-CNFET Current-Voltage characteristics

For the equilibrium situation considered in the previous section, computing the nanotube charge density involved a straightforward calculation of the self consistent potential profile. However, once a drain voltage is applied, the Schottky barrier profile at the drain end is modified as seen in the upper part of Fig.3.5. We must now account for the tunneling current through this barrier. The magnitude of the applied drain voltage not only causes the barrier height to reduce, but also induces an effective reduction in the

barrier width. Qualitatively, we can understand the effect of the drain voltage (assuming that the source is held to ground) on the current flowing through the nanotube as follows:

- Vds = 0: Initially when there is no voltage applied on the drain and only a positive gate voltage is applied, the band profile is as shown in Fig. 3.4. We observe identical Schottky barriers at the ends of the tube, the dimensions of which, are given by 3.8. The electrons from the source and drain can now tunnel through these barriers into the channel region and vice-versa. Although there is charge induced in the channel, there is no net current flow through the device since the electrochemical potentials at the source and drain are identical.

- $0 <$ Vds $<$ Vgs: As we start applying a positive potential at the drain, the electrochemical potential at the drain goes below the source and now the equilibrium is broken. The barrier at the drain end begins to diminish and electrons can easily tunnel out of the channel into the drain. The barrier dimensions at the source end, however, do not change. Thus, compared to the drain end of the tube, the electrons in the channel see a larger barrier at the source end and the flux of electron flowing into the source is far less than that flowing into the drain. In this regime of operation, the Fermi level of the nanotube can be considered to have split, giving rise to a quasi-Fermi level that describes the electron current. For the case Vds = Vgs, – shown in

the upper portion of Fig. 3.5 – the barrier at the drain is entirely suppressed and the backscattering of electrons at the drain end goes to zero. However, this means that it is also easier for electrons to flow into the channel from the drain end. This kind of negative flux has been considered in our model. It may be noted that, throughout the entire analysis, the mid-length Conduction Band Value of the channel does not change. It is held to its equilibrium value as decided by the gate potential. The channel band profile is entirely under the control of the gate.

- Vds > Vgs: When the voltage applied at the drain exceeds the gate voltage – shown in lower portion of Fig. 3.5 – a barrier spike begins to develop at the Valence band of the nanotube. This now presents the opportunity for holes to tunnel into the device from the drain. Thus, we now begin to see a hole component in the total current flowing through the device. Another effect is that as drain voltage is increased above the gate, the barrier width at the source end for the electrons begins to reduce. This can be explained as follows. The assumption of near ballistic transport through the nanotube implies that the net electron current flowing into the device from the source should equal the net electron current flowing out of the channel into the drain. Since the electron flow is determined only from the nature of the triangular

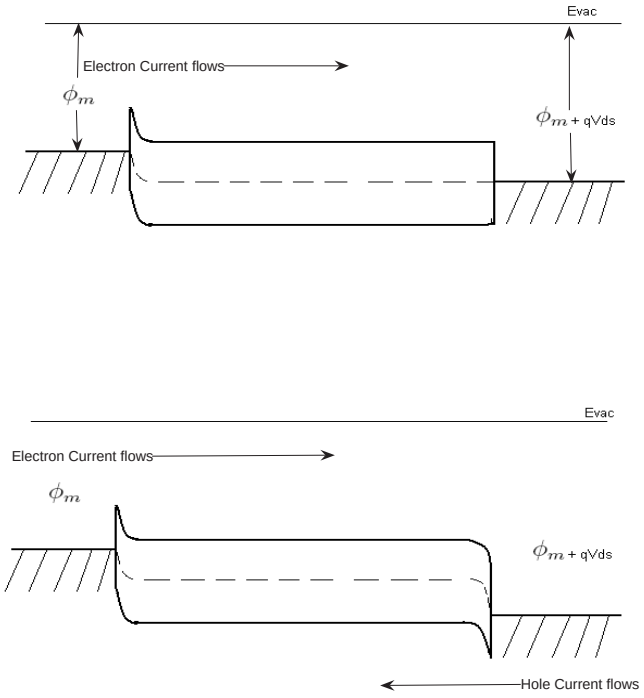

Figure 3.5: Non-Equilibrium Band profile
Suppressing the Schottky barrier at the drain (top). Formation of a tunneling barrier for holes (bottom)

barrier at the contacts, we can see that for a fixed barrier height at the source, an increase in the electron current can only be explained by a corresponding thickness in the barrier width.

- In addition to the current obtained as a function of the applied drain voltage, there is also a thermionic current component. This sets the limit for the minimum current flowing through the device.

From a study of the different modeling and simulation approaches for the SB-CNFET available in literature [11 - 14, 16 - 19], we concluded that the one best suited towards developing a compact model of the SB-CNFET for incorporation within a standard library was the approach adopted by Clifford et al.[10]. In order to model the current flowing through the SB-CNFET, we make use of the concept of quasi fermi levels for the electrons and holes, which can be used to compute the electron and hole current independently. This technique was adopted from [10].

3.4 Deriving expressions for transistor current

The current flowing through the channel of the SB-CNFET is derived from the standard two terminal Landauer conductance formula given by

$$I = \frac{q}{h} \int_{-\infty}^{+\infty} \bar{T}(E) \cdot [f(E - \mu_1) - f(E - \mu_2)] dE \tag{3.9}$$

where $\bar{T}$(E) is the composite quantum mechanical transmission coefficient through the ballistic device and fE is the Fermi-Dirac probability of an Energy state E being occupied. Here μ refers to the electrochemical potential at the source and drain end of the device under consideration.

For our model of the SB-CNFET, the Landauer equation can be modified

to obtain the electron current I_n from the equation:

$$\frac{2q}{\Pi\hbar}\int_{Ec}^{+\infty} T_s(E)\cdot[f(E)-f(E-E_{fn})]-T_d(E)\cdot[f(E-E_{fn})-f(E+qVds)]dE=0 \tag{3.10}$$

Here we are computing only the electron current contribution to the total current. Hence, the factor E_{fn} which is the electron quasi Fermi level. $T_s(E)$ and $T_d(E)$ are the quantum mechanical tunneling probabilities computed for the triangular Schottky barriers at the source and drain respectively. The factor 2 appears in the constant to account for the double degeneracy of the lowest sub-band.

The tunneling probability for a triangular barrier of height u and width l is given by the formula[5]

$$T_s=\exp(-\frac{4l}{9R}\sqrt{\frac{2u}{\Delta}}) \tag{3.11}$$

where Δ is half the value of the nanotube bandgap.

A similar current equation for the hole current I_p can be derived by expressing 3.10 in terms of the hole quasi Fermi levels as:

$$\frac{2q}{\Pi\hbar}\int_{+\infty}^{Ev} T_s(E)\cdot[f(E)-f(E+E_{fp})]-T_d(E)\cdot[f(E-qVds)-f(E+E_{fp})]dE=0 \tag{3.12}$$

The procedure for calculating the electron and hole currents is akin to the one for charge density calculation in the sense that, here also, a self consistent

solution to the quasi fermi levels and the net current flowing through the devices must be obtained. A starting point for computing the current is to calculate the tunneling probabilities at the source and drain using 3.11. The electron quasi Fermi level is initially referenced to the electrochemical potential of the source while the hole quasi Fermi level is referenced to the potential at the drain. We then iteratively solve the equations 3.10 and 3.12 using the Newton-Raphson method to obtain the self consistent solution to the electron and hole currents.

An expression for the Thermionic Current

The expression for the aggregate thermionic current – due to both electrons and holes – as a function of the applied drain voltage for a CNFET has been derived by Guo et. al. [25] and is given by:

$$I_t = \frac{8e^2}{h} \cdot \exp(-\frac{Eg}{2KT}) \cdot Vds \tag{3.13}$$

where h = Planck's constant, Eg is the nanotube bandgap and KT = 25.6 meV at 300K.

Therefore the total current flowing through the nanotube is given by

$$I = I_n + I_p + I_t \tag{3.14}$$

Chapter 4

Results and Analysis

The analytical expressions for the behavior of SB-CNFET were incorporated into a compact model and simulated for a SB-CNFET with the following parameters:

- SWNT Radius: Rt = 0.6nm
- SWNT Length: Lt = 100nm
- Gate Dielectric Thickness: Rg = 10*Rt = 6.6nm
- SWNT Work function = Source/drain/gate metal workfunction = 4.5eV
- Gate Insulator = Zirconia(Relative Dielectric constant = 16.1)
- Operating temperature = 300K

4.1 Nanotube Density of States

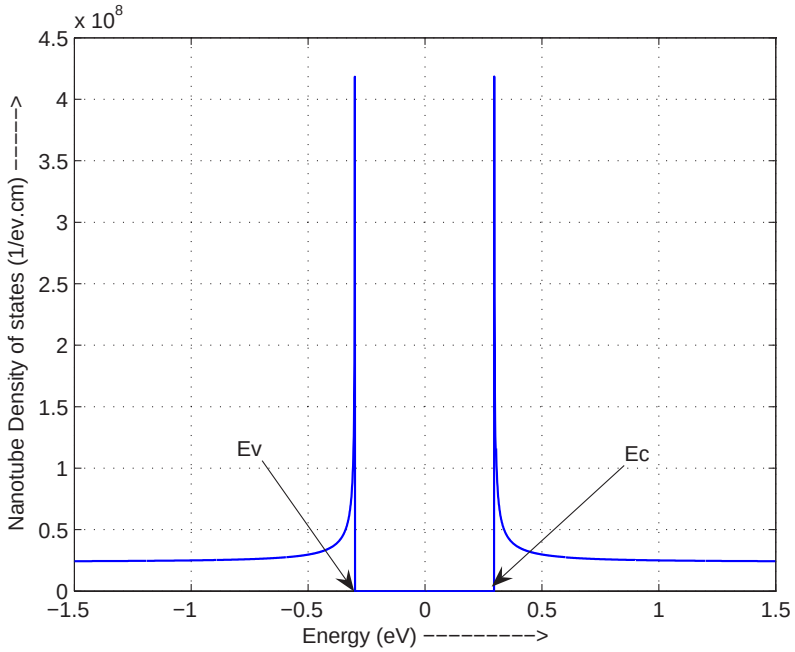

Figure 4.1: Density of States of the SWNT around the Fermi Level

The simulation of the DOS for the lowest sub-band of a typical SWNT shows a symmetric density of states around the Fermi level with the maxima at just above the conduction band and just below the valence band respectively as shown in Fig. 4.1.

The simulation of the SWNT in the SB-CNFET in our study is shown in Fig. 4.2. There is a spike just above the conduction band and an exponential decay beyond that with increasing energy.

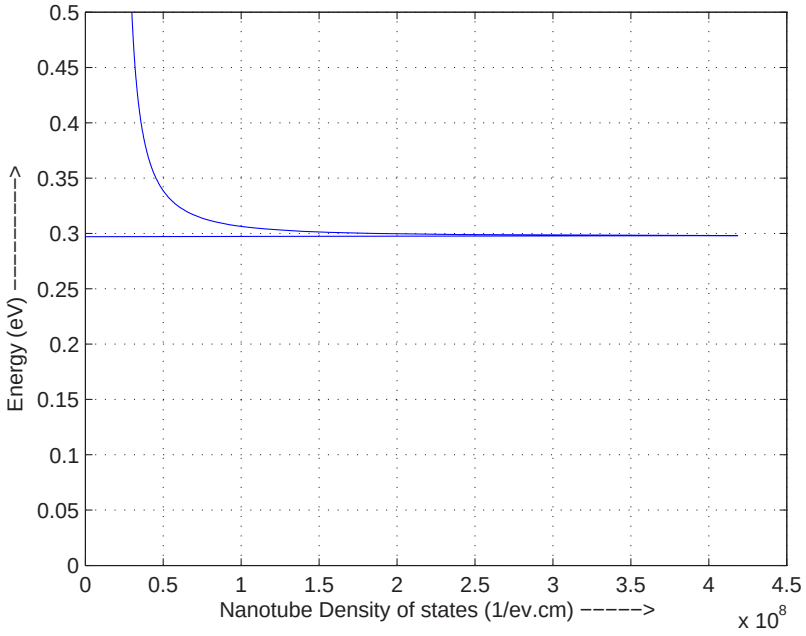

Figure 4.2: Density of States of the SWNT in the SB-CNFET studied

4.2 Equilibrium characteristics

The mid length charge induced on the nanotube is shown in Fig. 4.3. As expected, the charge increases with increasing gate voltage due to the gate capacitance relationship. The increase in the charge density is almost linear after 0.2 Volt.

Fig. 4.4 shows the result obtained for a coaxially gated SWNT by Guo et. al. in [19]. By comparison with Fig. 4.3, it can be seen that the two results show agreement.

The plot of the Conduction Band as a function of the gate voltage as shown in Fig. 4.5 shows that the conduction band is lowered due to an increase in gate voltage. However, the amount by which it is lowered reduces with increase in gate voltage. This is because an increase in the gate voltage produces a linear increase in the charge induced. This induced charge increases the gate dielectric capacitance and part of the gate voltage drops over this capacitor. This feature introduces the requirement for a self-consistent charge - band profile calculation. In fact, a comparison of Figs. 4.5 and 4.3 shows that for $Vgs \leq 0.2$ the charge density increases quadratically and the conduction band too shows much lowering. For higher values of Vgs, as more and more charge is induced, the gate dielectric capacitance increases greatly and we can observe the consequent effect of a reduced lowering of the conduction band edge.

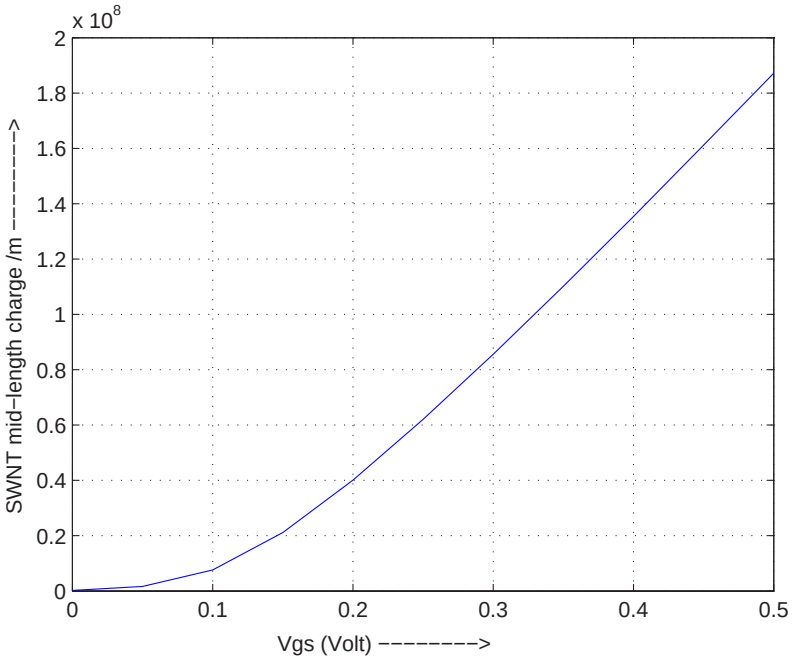

Figure 4.3: Charge Density on the SWNT as a function of the applied gate voltage

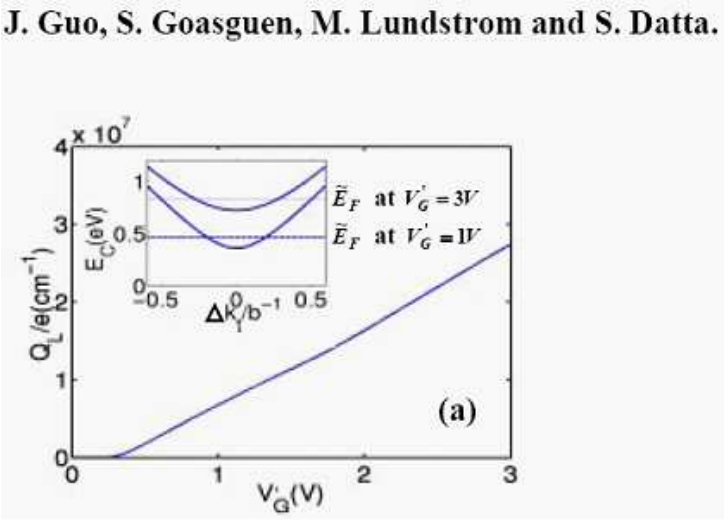

Figure 4.4: Charge Density on the SWNT computed by Guo et.al.

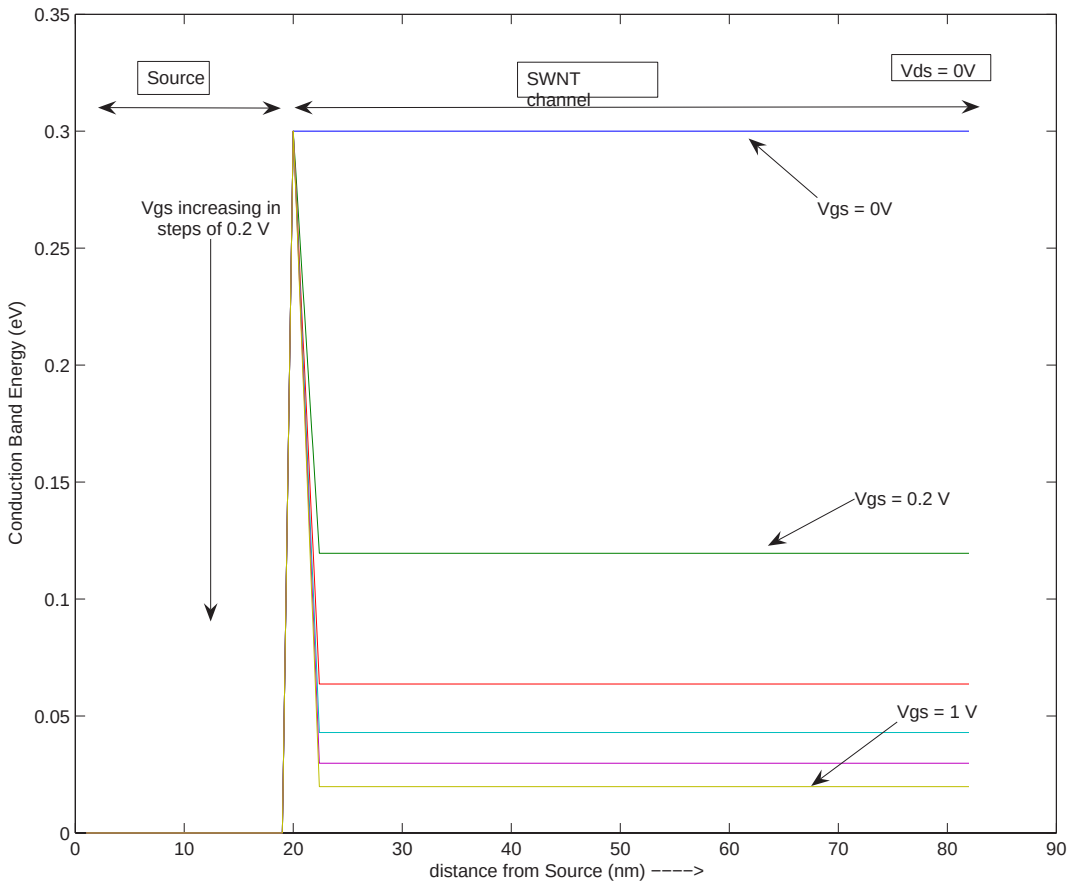

Figure 4.5: Conduction Band profile of the SB-CNFET as a function of the applied gate voltage

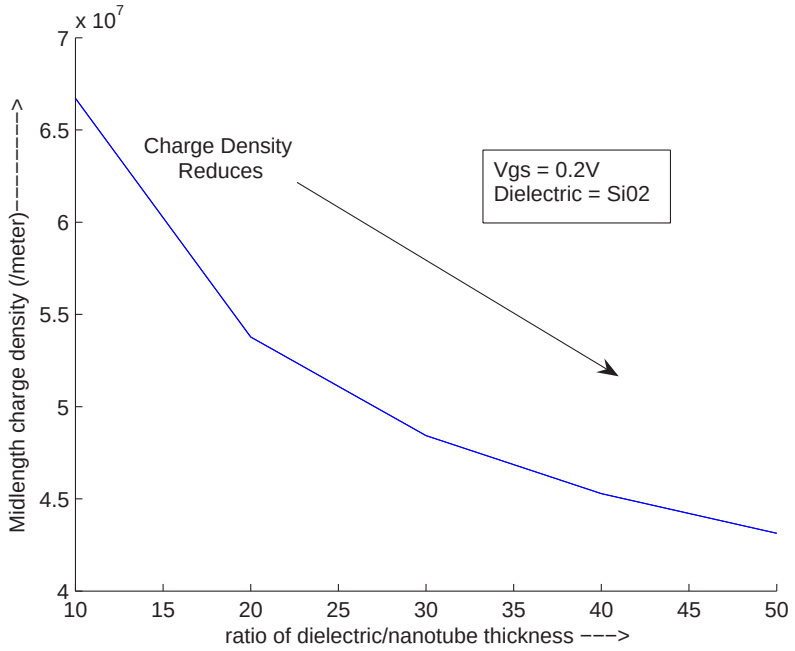

Figure 4.6: Charge induced on the gate as a function of dielectric thickness

4.2.1 Effect of Gate Insulator Thickness

Fig. 4.6 shows that as the ratio of the gate dielectric radius to the SWNT radius increases, the charge induced on the nanotube is reduced. This can be explained by the simple capacitance equation which states that the capacitance is inversely proportional to the distance between the plates. It follows that the charge induced on the channel must reduce for increasing thickness of the gate dielectric. This can simply be viewed as a reduction in the ability of the gate to control the channel as it is moved further away from it. Thus, as the gate dielectric is made thinner, the gate has better control over the

channel.

4.2.2 Effect of Gate Insulator Dielectric Constant

A higher dielectric constant of the gate insulator results in a higher gate capacitance and obviously this means that more charge will be induced on the nanotube. The Fermi level of the channel will be raised or there will relatively be an increased band bending. This simulated result is shown in Fig. 4.6. The gate dielectrics Silicon Dioxide ($\epsilon = 11.7$), Alumina ($\epsilon = 9.3$) and Zirconia ($\epsilon = 16.1$) are often used in CNFETs and have therefore been simulated for the SB-CNFET model under study.

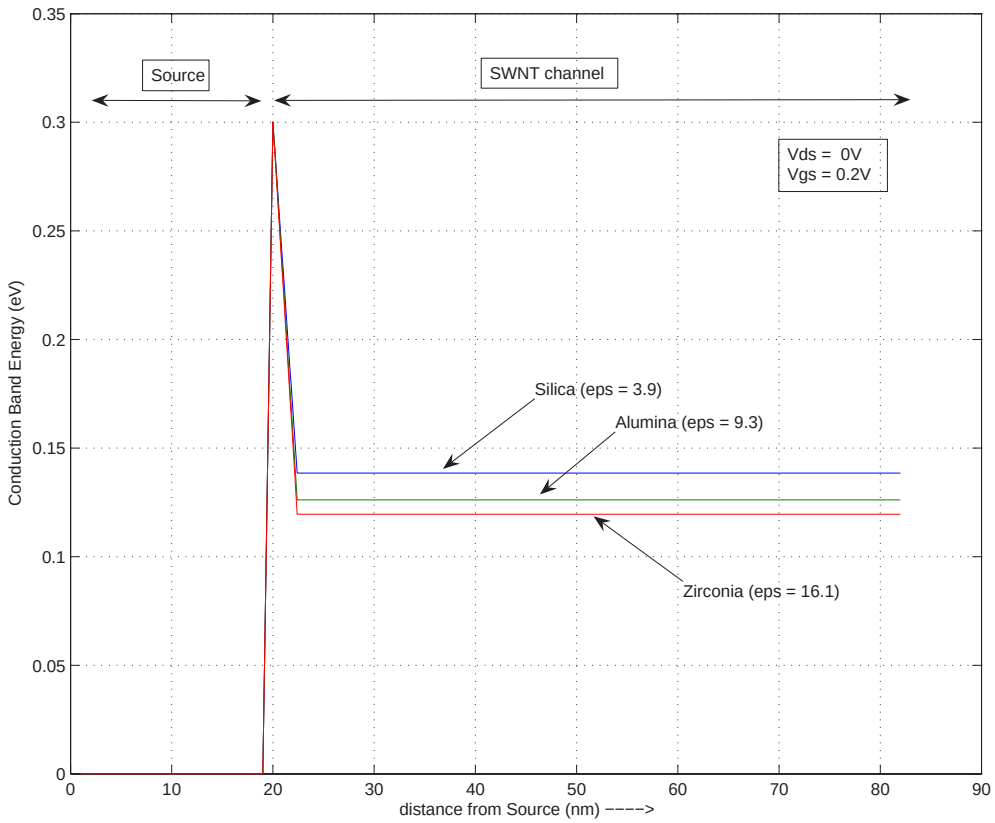

Figure 4.7: Conduction Band profile of the SB-CNFET for different dielectrics

4.3 The SB-CNFET under non-equilibrium

When a positive voltage is applied on the drain, the barrier spike begins to progressively diminish at that end of the channel. The barrier thickness, as seen by the charge carriers, begins to reduce too. Consequently, the electrons induced on the channel can now enter the drain metal by tunneling through the barrier while those carriers with sufficient thermal energy can jump over the barrier. The limiting value of current through the nanotube is described by the thermionic current component. This is shown in Figs. 4.8(a and b), which show the simulated I-V characteristics for small values of Vgs and Vds. We can see from the figure, that when no gate voltage is applied, the current is purely thermionic. For the case of Vgs = 0 in Fig. 4.8(a), the current increases linearly with Vds. This is attributed to the linear dependance of the thermionic current on the drain voltage. The application of a positive gate voltage induces heavy charge on the channel. It can be seen from the same figure that the current due to charge, tunneling through the barrier at the drain end, is significantly greater than the thermionic current component. The transfer characteristics in Fig. 4.8(b) reflect a similar scenario. For an applied drain voltage, the current increases almost quadratically as soon as a gate voltage is applied. The two drain and transfer characteristics show that the current flowing through the device is very sensitive to the drain voltage and is largely controlled by manipulating the barrier height at the contacts. In the model we have considered, the barrier height is approximately, 0.3 eV.

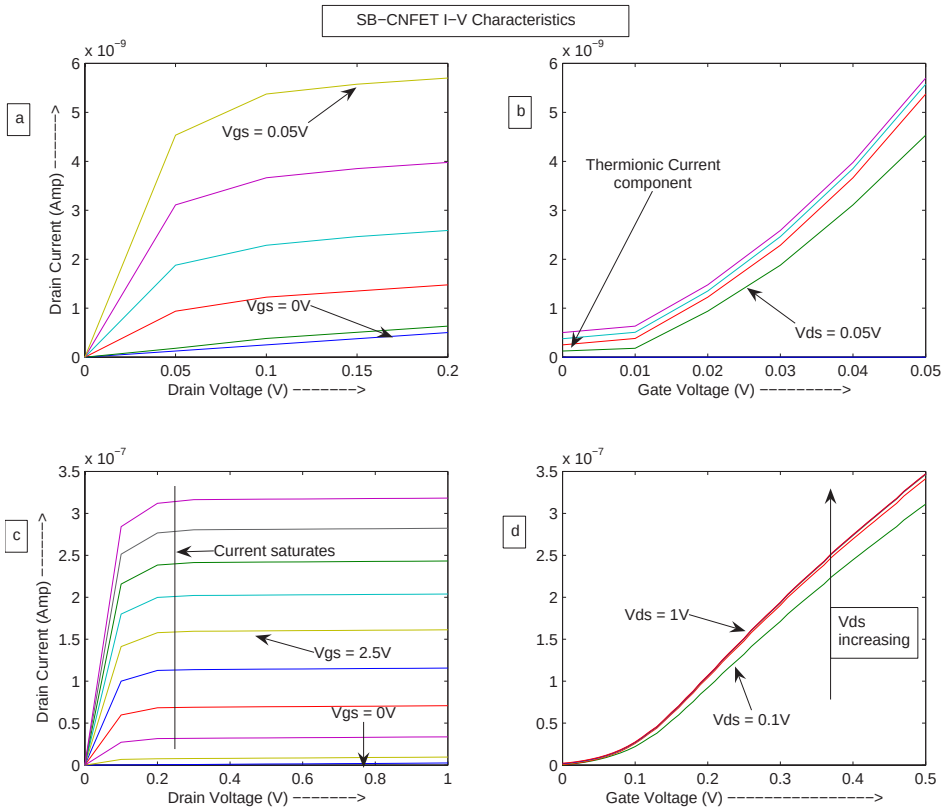

Figure 4.8: Unipolar I-V characteristics of the SB-CNFET

We can see from Fig. 4.8(c) that for a given Vgs, the current saturates at approximately this region, i.e., when the applied Vds $\simeq$ barrier height. At this point the barrier is entirely suppressed and there is maximum current flow through the channel. Fig. 4.8(d) shows an almost linear increase in the current as a function of the gate voltage. The onset of current saturation as a function of drain voltage is expressed very clearly here. The plot (d) consists of 5 curves for Vds ranging from 0 - 1 V. However, while there is a marked increase in the current for an increase of Vds from 0.1V to 0.3V, beyond this limit, all the other curves representing the higher values of Vds are almost merged. The electron current beyond this point is independent of Vds.

Bipolar Current Characteristics

The simulation results shown in Fig. 4.8 can now be extended to include contribution due to the hole current. As the drain voltage is increased beyond the half bandgap value of SWNT, the barrier for electrons at the drain is entirely suppressed and now a tunneling barrier begins to form for the holes. This leads to a net bipolar current that has contribution from the electrons injected into the channel from the source as well as holes injected into the channel from the drain. At this point, the fermi level obtained by self consistent calculation of the gate potential is insufficient to describe both types of carriers. The Fermi level is now described by a quasi fermi level for the electrons (referenced to the source) and a quasi fermi level for the holes (referenced to the drain). As Vds keeps increasing, the hole current begins to increase until the point where Vds = valence band edge of the SWNT. At this point, the contribution due to the hole current equals that of the electron current and for a higher Vds, the hole current exceeds the electron current in magnitude. This is shown in Fig. 4.9. Fig. 4.10 shows the Bipolar I-V characteristics for a SB-CNFET obtained by Clifford et al in their study [10]. It can be seen by comparison with our results in Fig. 4.9, that the graphs are very similar in nature, especially graphs 3 and 4 of their study.

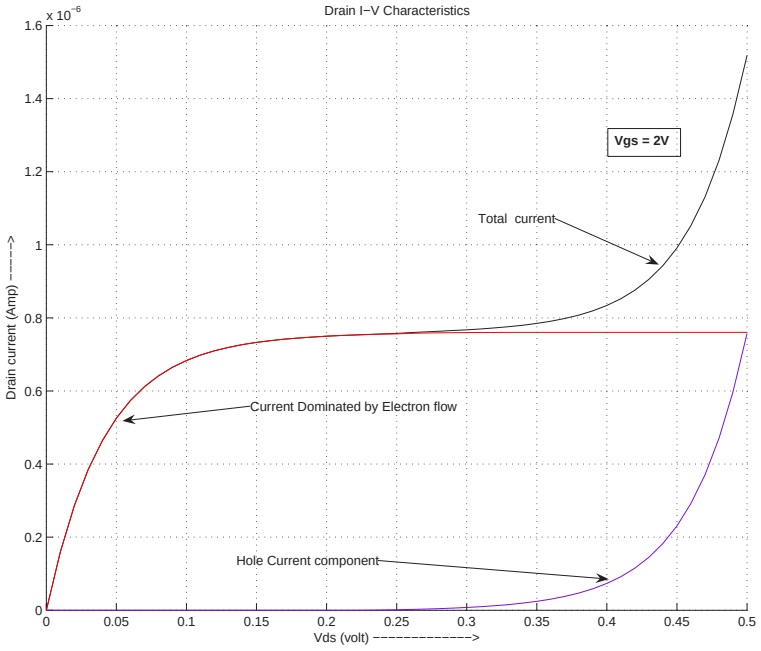

Figure 4.9: Bipolar I-V characterisitcs of the SB-CNFET

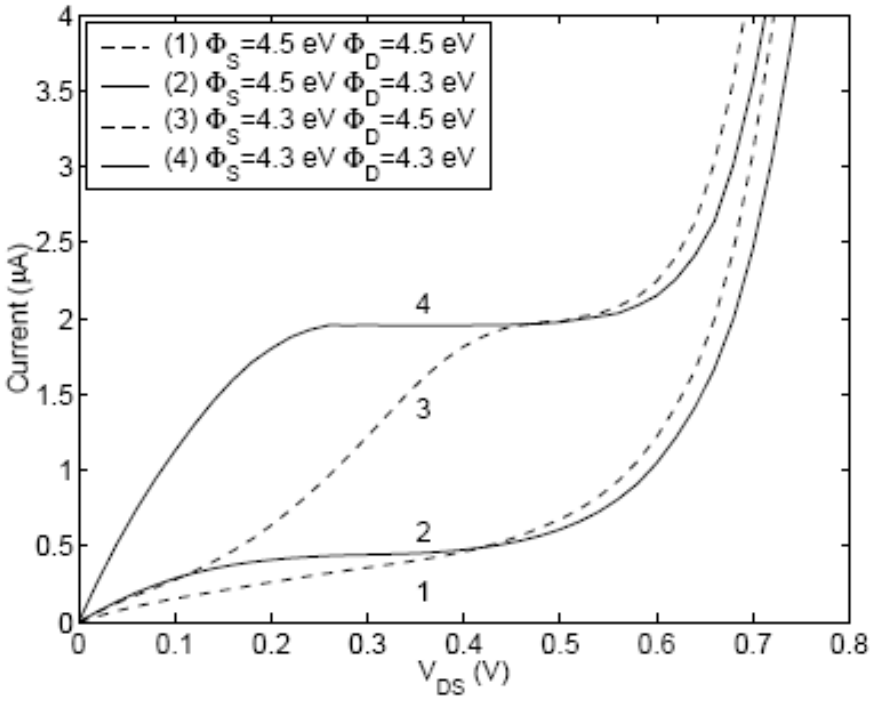

Figure 4.10: Bipolar I-V characterisitcs of the SB-CNFET from [10]

Chapter 5

Conclusions and Future Work

In summary, a compact model was developed for the Schottky-Barrier Carbon Nanotube Field Effect Transistor with the following key concepts

- 1-D nanotube density of states
- Self-consistent band profile computation
- Assumption of ballistic transport and use of Landauer formalism for current expression
- Triangular Barrier Approximation
- Use of quasi-fermi levels to account for bipolar current flow
- Thermionic current

This model was implemented in MATLAB as a collection of scripts and functions and can be incorporated as a library in any standard Hardware Description language. When simulated in MATLAB, this model adequately explains the working of the SB-CNFET and demonstrates the bipolar nature of current flow in the transistor. It also accounts for the thermionic (leakage) current through the device and can generate the transistor I-V characteristics and their dependance on the gate dielectric thickness and nature of the insulator used.

Scope for future work

The model developed in this thesis work can be improved upon by determining the electrostatics at the contacts and doing away with the triangular barrier approximation. Also, phonon scattering within the device can be taken into consideration. However, the incorporation of phonon scattering effects might increase the complexity if computed in real space. The techniques used by Guo in [25] for mode space approach can be actively investigated for improving the accuracy of the model while maintaining its compactness.

The compact model developed in the thesis can be used to model circuits composed of CNTs such as basic inverters and logic gates. The various parameters such as the contact work functions, gate dielectrics etc., can be tweaked to obtain the desired geometry of SB-CNFET based on the application.

Bibliography

[1] Iijima, S. "Helical Microtubules of Graphitic Carbon," *Nature,* V. 354, pp. 56–58, 1991.

[2] Sheu, B.; Chung-Yu Wu, P; and Sze, S.M. "Scanning the Issue," *in Proc. of the IEEE,* V. 91, No. 11, Nov. 2003.

[3] http://mmptdpublic.jsc.nasa.gov/jscnano

[4] Avouris, P.; Appenzeller, J.; Martel, R.; and Wind, S.J. "Carbon Nanotube Electronics," *in Proc. of the IEEE,* V. 91, No. 11, Nov. 2003.

[5] Odintsov, A.A. "Schottky Barriers in Carbon Nanotube Heterojunctions," *Physics Review Letters,* V. 85, No. 1, pp. 150–153, Jul. 2000.

[6] Ungersböck, E., et. al. "Simulation of Carrier Transport in Carbon Nanotube Field Effect Transistors," *in Proc. of the IEEE,* V. 91, No. 11, Nov. 2003.

[7] Guo, J; Datta, S.; and Lundstrom, M; "Towards Multi-Scale Modeling of Carbon Nanotube Transistors ," *Applied Physics Letters,* V. 81, No. 8, pp. 1486–1488, Aug. 2002.

[8] Frank, S. et al. "Carbon Nanotube Quantum Resistors," *Science,* V. 280, June. 1998.

[9] Luryi, S. "Quantum Capacitance Devices," *Applied Physics Letters,* V. 52, pp. 501–503, June. 1988.

[10] Clifford, J.P.;John, D.L.; and Pulfrey, D.L. "Bipolar Conduction and Drain-Induced Barrier thinning in Carbon Nanotube FETs," *IEEE Trans. on Nanotechnology,* V. 2,No. 3, pp. 181–185, Sept. 2003.

[11] Clifford, J.P.; John, D.L.; and Pulfrey, D.L. "Electrostatics of Coaxial Schottky-Barrier Nanotube Field-Effect Transistors ," *IEEE Trans. Electron Dev,* V. 2,No. 3, pp. 175–180, Sept. 2003.

[12] Castro, L.C.; John, D.L.; and Pulfrey, D.L. "An Improved Evaluation of the DC Performance of the Carbon Nanotube Field-Effect Transistors ," *Smart Materials and Systems,* Aug. 2004.

[13] John, D.L.; Castro, L.C.; Pereira, P.J.S. and Pulfrey, D.L "A Schrödinger-Poisson Solver for Modelling Carbon Nanotube FETs ," *in Proc. NSTI Nanotech.* , V. 3, pp. 65-68, 2004.

[14] Clifford, J.P.; John, D.L.; Castro, L.C; and Pulfrey, D.L. "Electrostatics of Partial Gated Carbon Nanotube FETs," *IEEE Trans. on Nanotechnology*, V. 3,No. 2, pp. 281–286, June. 2004.

[15] Derycke, V.; Martel, R.; Appenzeller, J.; Avouris, P. "Carbon Nanotube Inter- and IntraMolecular Logic Gates," *IEEE Trans. on Nanotechnology*, V. 1, No. 9, Aug. 2001.

[16] Dwyer, C.; Cheung, M.; and Sorin, D.J. "Semi-empirical SPICE Models for Carbon Nanotube FET Logic," *in Proc. of the 4th IEEE Conference on Nanotechnology*, pp. 386–388, Aug. 2004.

[17] Burke, P.J."AC Performance of Nanoelectronics: towards a Ballistic THz Nanotube Transistor," *Solid State Electronics* , March. 2004.

[18] Burke, P.J."An RF Circuit Model for Carbon Nanotubes," *IEEE Trans. on Nanotechnology*, V. 2, No. 1, March. 2003.

[19] Guo, J; Goasguen, S; Lundstrom, M; and Datta, S. "Metal-Insulator-Semiconductor Electrostatics of Carbon Nanotubes ," *Applied Physics Letters*, V. 81, No. 8, pp. 1486–1488, Aug. 2002.

[20] Guo, J; Datta, S.; and Lundstrom, M; "A Numerical Study of Scaling Issues for Schottky Barrier Carbon Nanotube Transistors," *IEEE Trans. on Nanotechnology,*, V. 51, No. 2, pp. 172–177, Feb. 2004.

[21] Guo, J; Lundstrom, M; and Datta, S. "Performance Projections for Ballistic Carbon Nanotube Field-Effect Transistors," *Applied Physics Letters*, V. 80, No. 17, pp. 3192–3194, 2002.

[22] Mintmire, J.W; and White, C.T. "Universal Density of States for Carbon Nanotubes," *Physics Review Letters*, V. 81, No. 12, pp. 2506–2509, Sep. 1998.

[23] Guo, J., et. al. "Assessment of Silicon MOS and Carbon Nanotube FET Performance Limits Using a General Theory of Ballistic Transistors," *IEDM Tech. Digest*, pp. 711–714, Dec. 2002.

[24] Datta, S. *Quantum Transport: Atom to Transistor*. Cambridge; New York: Cambridge University Press, 2005.

[25] Guo, J. *Carbon Nanotube Electronics: Modeling, Physics and Applications*. Ph.D. Thesis submitted to Purdue University, Aug. 2004.

[26] www.nanotech-now.com/.../issues/011/011.htm

Matlab scripts and functions used in simulating the SB-CNFET

```
% Nanotube 1-D Density of states per Joule-meter computation
%-------------------------------------------------------------

function density_of_states = D(E)
h = 6.625E-34; pi = 3.1314; hbar = h/(2*pi);q = 1.6E-19; %J
%Fermi velocity of electron
vf = 8.1E5;%m/s
% Nanotube radius
r = 0.6E-9; %nm
% Nanotube Bandgap
Eg = 2*hbar*vf/(3*r*q); delta = Eg/2;%eV

const1 = 4/(pi*hbar*vf);% constant in the equation (1/joule-meter)
density_of_states = const1 * theta(abs(E)-delta)*abs(E)/sqrt(E^2 - delta^2);

function stepfunction = theta(E); %subfunction
if E>=0
    stepfunction = 1;
else stepfunction = 0;
end
```

```
% This function computes the fermic-dirac probability if a state being
% filled by electrons
%-------------------------------------------------------------------------
function fermi_dirac_probability = f(E)
kT = 0.0256;
Ef = 0;
fermi_dirac_probability = 1/(1+exp(E-Ef/kT));

% Script for calculating density of states in a CNT both on the Conduction
% and Valence band
%-------------------------------------------------------------------------
volt = 0;
for energy = -1.5:0.001:1.5
    volt =volt+1;
    Q(volt) = D(energy);
    energyrange(volt) = energy;
end
density = Q * 1.6E-19/1E2;% DOS in 1/(ev-cm)
h = plot(energyrange, density);
set(h,'linewidth',[1.0]);
```

```
ylabel ( 'Nanotube Density of states (1/ev.cm) ----->');
xlabel ('Energy (eV) --------->');
grid on;



% Script for calculating density of states in the SWNT under test
%-----------------------------------------------------------------
index = 0;% dummy variable for generating an array
% The Fermi level of the tube is set to 0 by grounding the source and drain
% The work functions of the metal and charge neutrality level of nanotube
% are assumed to be of the same value

% Evaluation of Density of states from 0 to 0.5 eV
for Energy = 0:0.001:0.5
    index =index+1;
    density(index) = D(Energy); % DOS calculated by function D(E)
    Energyrange(index) = Energy;
end
density = density * 1.6E-19/1E2;% conversion from 1/(J-m) to 1/(eV-cm)
plot(density, Energyrange);
%set(h,'linewidth',[2.0]);
xlabel ( 'Nanotube Density of states (1/ev.cm) ----->');
```

```
ylabel ('Energy (eV) ---------->');
grid on;
```

```
% Script to determine the charge density for different values of Vgs
%-----------------------------------------------------------------
clear all
clc

eps = 3.9*8.85E-12; %dielectric permittivity farad/m (16.1 for zirconia)
tdiel = 6E-9;%dielectric thickness in meter
dicap = 6.28*eps/log(6.6/0.6);%dielectric capacitance for concentric
                                cylinders in F/m

%Energy by which the conduction band moves upwards by addition of a single
%electron
Usingle = 1.6E-19/dicap;% eV-meter of energy per electron added

% Computation of the self consistent field for different Vgs
%-----------------------------------------------------------
index = 0;
for Vgs = 0:0.05:0.5; %Applied gate voltage
    index =index+1; %some variable for use as index in array
    U = 0; %Mid-length Self Consistent Field
    dU = 1;%some initial value of error
     while dU>1E-5
```

```
        iterationcount = iterationcount+1;
        charge = 0;
        for Energy = 0:0.01:1 %integrating from 0 to 1eV
            charge = charge + (D(Energy)*1.6E-19)*f(Energy-Vgs+U);
            %total charge per meter
        end
        Unew = charge*Usingle;
        %potential energy for given charge density in eV
        dU = abs(U-Unew); %error in computation
        U = U + 0.01*(Unew-U);
    end
    Energyrange(index) = Vgs;%Vgs(V)
    totalcharge(index) = charge;%charge per meter
end


% Plot of charge induced as a function of Gate Voltage
% ----------------------------------------------------
hold on
g = plot(Energyrange, totalcharge);
xlabel('mid-length charge /m');
ylabel('Vgs (Volt)--------> ');
```

```
% Script to generate CB profiles for different values of Vgs. The CB goes
% down as Gate Voltage is applied.
%------------------------------------------------------------------------
clear all
clc

eps = 16.1*8.85E-12; %dielectric permittivity farad/m (16.1 for zirconia)
tdiel = 6E-9;%dielectric thickness in meter
Rg = 2.4; Rt = 0.6; %gate dielectric thickness and nanotube radius in nanometer
dicap = 6.28*eps/log(Rg/Rt);%dielectric capacitance for concentric cylinders in

%Energy by which the conduction band moves upwards by addition of a single
%electron
Usingle = 1.6E-19/dicap;% eV-meter of energy per electron added

% Computation of the self consistent field for different Vgs
%-------------------------------------------------------------
index = 0;
for Vgs = 0:0.2:1; %Applied gate voltage
    index =index+1; %some variable for use as index in array
    U = 0; %Mid-length Self Consistent Field
    dU = 1;%some initial value of error
```

```
iterationcount = 0;
while dU>1E-5
    iterationcount = iterationcount+1;% counter to prevent infinite loop
    charge = 0;
    for Energy = 0:0.01:0.5 %integrating from 0 to 0.5eV
        charge = charge + (D(Energy)*1.6E-19)*f(Energy-Vgs+U);
                                        %total charge per meter
    end
    Unew = Usingle * charge/(2*3.14*0.6); %potential energy for given
                                            charge density in eV
    dU = abs(U-Unew); %error in computation
    U = U + 0.01*(Unew-U);
    if iterationcount > 50000, break, end
end
Energyrange(index) = Vgs;%Vgs(V)
totalcharge(index) = charge;%charge per meter

% Computation and Plot of the Conduction and Valence Band Profiles
% ---------------------------------------------------------------
index1 = 19; %dummy variable for array index
for i = 1:20
    length(i) = i;
    conduction_band_value(index,i) = 0;
```

```
    end
    for i = 0:0.1:Rg %Running along length of tube from 0 to Rg
        index1 = index1 + 1;% first 19 index values of the array
                            reserved for metal work function
        length(index1) = 20+i;
        conduction_band_value(index, index1) = 0.3-(Vgs-U)*(i/Rg);
    end
    for i = 1:50 %CB profile from Rg to midlength
        length(index1+i) = 20+12+i;
        conduction_band_value(index, index1+i) = 0.3 - (Vgs-U);
    end
end
    valence_band_value = conduction_band_value-0.6;
    plot(length, conduction_band_value);
    xlabel('distance from Source (nm) ---->');
    ylabel('Conduction Band Energy (eV)');
```

```
% Script to generate CB profiles for different dielectric materials. The CB
% goes down as as the Permittivity of the Gate dilectric increases because
% more charge is induced due to increase in the gate capacitance.
%-------------------------------------------------------------------------

clear all
clc

for i = 1:1:3
    if i == 1
        eps = 3.9*8.85E-12; %dielectric permittivity farad/m (3.9 for Silica)
    else if i == 2
        eps = 9.3*8.85E-12; %dielectric permittivity farad/m (9.3 for Alumina)
        else
           eps = 16.1*8.85E-12; %dielectric permittivity farad/m (16.1 for zirc
        end
    end
    tdiel = 6E-9;%dielectric thickness in meter
    Rg = 2.4; Rt = 0.6; %gate dielectric thickness and nanotube radius in nanom
    dicap = 6.28*eps/log(Rg/Rt);%dielectric capacitance for concentric cylinder

    %Energy by which the conduction band moves upwards by addition of a single
    %electron
```

```
Usingle = 1.6E-19/dicap;% eV-meter of energy per electron added

% Computation of the self consistent field for different Vgs
%-------------------------------------------------------------
index = 0;
Vgs = 0.2; %Applied gate voltage
index =index+i; %some variable for use as index in array
U = 0; %Mid-length Self Consistent Field
dU = 1;%some initial value of error
iterationcount = 0;
while dU>1E-5
    iterationcount = iterationcount+1;% counter to prevent infinite loop
    charge = 0;
    for Energy = 0:0.01:0.5 %integrating from 0 to 0.5eV
        charge = charge + (D(Energy)*1.6E-19)*f(Energy-Vgs+U);
    end
    Unew = Usingle * charge/(2*3.14*0.6);
    dU = abs(U-Unew); %error in computation
    U = U + 0.01*(Unew-U);
    if iterationcount > 50000, break, end
end
Energyrange(index) = Vgs;%Vgs(V)
totalcharge(index) = charge;%charge per meter
```

```
    % Computation and Plot of the Conduction and Valence Band Profiles
    % ---------------------------------------------------------------
    index1 = 19; %dummy variable for array index
    for i = 1:20
        length(i) = i;
        conduction_band_value(index,i) = 0;
    end
    for i = 0:0.1:Rg %Running along length of tube from 0 to Rg
        index1 = index1 + 1;%
        length(index1) = 20+i;
        conduction_band_value(index, index1) = 0.3-(Vgs-U)*(i/Rg);
    end
    for i = 1:50 %CB profile from Rg to midlength
        length(index1+i) = 20+12+i;
        conduction_band_value(index, index1+i) = 0.3 - (Vgs-U);
    end
end

valence_band_value = conduction_band_value-0.6;
plot(length, conduction_band_value);
xlabel('distance from Source (nm) ---->');
ylabel('Conduction Band Energy (eV)');
```

```
% Script to determine the charge density for different values of dielectric
% thickness ratios for a fixed value of Vgs
%-------------------------------------------------------------------------
clear all
clc

eps = 3.9*8.85E-12; %dielectric permittivity farad/m (16.1 for zirconia)


% Computation of the self consistent field for different Thickness ratios
%-------------------------------------------------------------------------
index = 0;
Vgs = 0.2;%Volt
for thickness_ratio = 10:10:50 % varying the thickness ratio of Rg/Rt from 10 t
    dicap = 6.28*eps/log(thickness_ratio);
    %dielectric capacitance for concentric cylinders in F/m

    %Energy by which the conduction band moves upwards by addition of a single
    %electron
    Usingle = 1.6E-19/dicap;% eV-meter of energy per electron added

    index =index+1; %some variable for use as index in array
    U = 0; %Mid-length Self Consistent Field
```

```
    dU = 1;%some initial value of error
    while dU>1E-5
        charge = 0;
        for Energy = 0:0.001:0.5 %integrating from 0 to 0.5eV
            charge = charge + (D(Energy)*1.6E-19)*f(Energy-Vgs+U);
            %total charge per meter
        end
        Unew = charge*Usingle; %potential energy for given charge density in eV
        dU = abs(U-Unew); %error in computation
        U = U + 0.1*(Unew-U);
    end
    MidlengthEnergy(index) = U;
    %Conduction band value for Vgs=0.2V for different thickness ratios
    totalcharge(index) = charge;%charge per meter for different thickness ratio
    thicknessratiorange(index) = thickness_ratio;
end



% Plot of charge induced as a function of Dielectric thickness for Vgs=0.2V
% ------------------------------------------------------------------------
hold on
g = plot(thicknessratiorange, totalcharge);
xlabel('ratio of dielectric/nanotube thickness --->');
```

```
ylabel('Midlength charge density (/meter)--------> ');
grid on
```

```
% To calculate Drain current vs Dain voltage for different Vgs for both the
% subthreshold as well as above threshold case
% ------------------------------------------------------------------------


clear all;
clc;


pi = 3.1314;
h = 6.625E-34; % J-s (Planck's constant)
hbar = h /(2*pi);
KT = 0.0256;%eV
q = 1.6E-19; %couloumb

%dielectric permittivity farad/m (16.1 for zirconia)
eps = 16.1*8.85E-12;
%gate dielectric thickness and nanotube radius in nanometer
Rg = 6; Rt = 0.6;
%Fermi velocity of electron
vf = 8.1E5;%m/s

% Nanotube Bandgap
Eg = 2*hbar*vf/(3*Rt*1E-9*q); delta = Eg/2;
```

```
%dielectric capacitance for concentric cylinders in F/m
dicap = 2*pi*eps/log(Rg/Rt);

%Energy by which the conduction band moves upwards by addition of a single
%electron
Usingle = 1.6E-19/dicap;% eV-meter of energy per electron added

% phicn = phig =4.5;% Carbon nanotube and gate metal work functions (eV)
% phis = phid = 4.63;% Source and Drain metal workfunctions (eV)

%---------------------------------
%*******Sub-Threshold************
%---------------------------------

% Computation of the mid length self consistent field for a given Vgs
%--------------------------------------------------------------------
indexVgs=0;
for Vgs = 0:0.01:0.05; %Applied gate voltage (volt)
    indexVgs = indexVgs+1;%index variable for array
    U = 0; %Mid-length Self Consistent Field
    dU = 1;%some initial value of error
    while dU>1E-5
        charge = 0;
```

```
    for Energy = 0:0.01:0.5 %integrating from 0 to 0.5eV
        charge = charge + (D(Energy)*1.6E-19)*f(Energy-Vgs+U);
    end
    Unew = charge*Usingle; %potential energy for given charge density in eV
    dU = abs(U-Unew); %error in computation
    U = U + 0.01*(Unew-U);
end

%Computation of the VI characteristics by self consistent procedure
%-------------------------------------------------------------------
%This procedure involves calculating the barrier heights from the
%equilibrium Conduction band profile and then obtaining the transmission
%probabilities from them. Each of these probabilities is multiplied with
%the corresponding fermi function over the entire conduction band range

indexVds = 0;
for Vds = 0:0.05:0.2;%Drain voltage (volt)
    indexVds = indexVds + 1;

    % Assume a quasi fermi level for electrons : set to charge neutrality l
    % - Vgs + Uscf computed above
    Efn = 0;
    CB = delta - Vgs + U;
```

```
% The Fermi function at Source contact is f(E) while within the nanotub
% shifts to f(E-Efn) and at the drain contact, it is f(E-q*Vds)

% Self-consistent current calculation
%-----------------------------------
dEf = 1;
count=0;% counter
while abs(dEf) > 1E-5
    flux1= 0; flux2= 0; flux3= 0; flux4 = 0;
    for E = CB:0.01:delta
        %Source barrier height(hs) and width(ws) in nm
        hs = delta - E; ws = (Rg-Rt)*(delta-E)/(delta-CB);
        %Drain barrier height (hd) and width (wd) in nm
        hd = delta - Vds - E; wd = (Rg-Rt)*(delta-Vds-E)/(delta-Vds-CB)
        flux1 = flux1 + T(hs,ws)*f(E);
        flux2 = flux2 + T(hs,ws)*f(E-Efn);
        flux3 = flux3 + T(hd,wd)*f(E-Efn);
        flux4 = flux4 + T(hd,wd)*f(E+Vds);
    end
    dEf = (flux1-flux2)-(flux3-flux4);
    Efn = Efn + sign(dEf)*0.001;
    count = count + 1;
```

```
            if count>500, break, end;
        end

        %Landauer formula for ballistic current. The additional q is to convert
        %to units of eV
        thermionic_current = (8*q^2/h) * exp(-0.3/KT) *Vds;%Amp
        electron_current(indexVgs, indexVds) = 2*(1.6E-19)^2/(pi*hbar) * (flux1
                                                + thermionic_current;
        drain_voltage(indexVds) = Vds;
    end

    gate_voltage(indexVgs) = Vgs;
end

subplot(2,2,1), plot(drain_voltage, electron_current);
xlabel('Drain Voltage (V) ------->');
ylabel('Drain Current (Amp) ------>');
subplot(2,2,2), plot(gate_voltage, electron_current);


% Computation of the mid length self consistent field for a given Vgs
%-----------------------------------------------------------------------
indexVgs=0;
```

```
for Vgs = 0:0.01:0.5; %Applied gate voltage (volt)
    indexVgs = indexVgs+1;%index variable for array
    U = 0; %Mid-length Self Consistent Field
    dU = 1;%some initial value of error
    while dU>1E-5
        charge = 0;
        for Energy = 0:0.01:0.5 %integrating from 0 to 0.5eV
            charge = charge + (D(Energy)*1.6E-19)*f(Energy-Vgs+U);
        end
        Unew = charge*Usingle; %potential energy for given charge density in eV
        dU = abs(U-Unew); %error in computation
        U = U + 0.01*(Unew-U);
    end

    %Computation of the VI characteristics by self consistent procedure
    %-------------------------------------------------------------------
    %This procedure involves calculating the barrier heights from the
    %equilibrium Conduction band profile and then obtaining the transmission
    %probabilities from them. Each of these probabilities is multiplied with
    %the corresponding fermi function over the entire conduction band range

    indexVds = 0;
    for Vds = 0:0.1:1;%Drain voltage (volt)
```

```
indexVds = indexVds + 1;

% Assume a quasi fermi level for electrons : set to charge neutrality l
% - Vgs + Uscf computed above
Efn = 0;
CB = delta - Vgs + U;

% The Fermi function at Source contact is f(E) while within the nanotub
% shifts to f(E-Efn) and at the drain contact, it is f(E-q*Vds)

% Self-consistent current calculation
%-----------------------------------
dEf = 1;
count=0;% counter
while abs(dEf) > 1E-5
    flux1= 0; flux2= 0; flux3= 0; flux4 = 0;
    for E = CB:0.01:delta
        %Source barrier height(hs) and width(ws) in nm
        hs = delta - E; ws = (Rg-Rt)*(delta-E)/(delta-CB);
        %Drain barrier height (hd) and width (wd) in nm
        hd = delta - Vds - E; wd = (Rg-Rt)*(delta-Vds-E)/(delta-Vds-CB)
        flux1 = flux1 + T(hs,ws)*f(E);
        flux2 = flux2 + T(hs,ws)*f(E-Efn);
```

```
            flux3 = flux3 + T(hd,wd)*f(E-Efn);
            flux4 = flux4 + T(hd,wd)*f(E+Vds);
        end
        dEf = (flux1-flux2)-(flux3-flux4);
        Efn = Efn + sign(dEf)*0.001;
        count = count + 1;
        if count>500, break, end;
    end

    %Landauer formula for ballistic current. The addition q is to convert h
    %to units of eV
    thermionic_current = (8*q^2/h) * exp(-0.3/KT) *Vds;%Amp
    electron_current(indexVgs, indexVds) = 2*(1.6E-19)^2/(pi*hbar) * (flux1
                                          + thermionic_current;
    drain_voltage(indexVds) = Vds;
end

gate_voltage(indexVgs) = Vgs;
end
subplot(2,2,3), plot(drain_voltage, electron_current);
xlabel('Drain Voltage (V) ------->');
ylabel('Drain Current (Amp) ------>');
subplot(2,2,4), plot(gate_voltage, electron_current);
```

```
% Electron Current as well as Hole current
% Script to generate CB and VB profiles and to compute the I-V
% characteristics the for different values of Vgs and Vds
%-----------------------------------------------------------------------
clear all;
clc;

pi = 3.1314;
h = 6.625E-34; % J-s (Planck's constant)
hbar = h /(2*pi);
q = 1.6E-19; %couloumb

%dielectric permittivity farad/m (16.1 for zirconia)
eps = 16.1*8.85E-12;
%gate dielectric thickness and nanotube radius in nanometer
Rg = 6.6; Rt = 0.6;
%Fermi velocity of electron
vf = 8.1E5;%m/s

% Nanotube Bandgap
Eg = 2*hbar*vf/(3*Rt*1E-9*q); delta = Eg/2;

%dielectric capacitance for concentric cylinders in F/m
```

```
dicap = 2*pi*eps/log(Rg/Rt);

%Energy by which the conduction band moves upwards by addition of a single
%electron
Usingle = 1.6E-19/dicap;% eV-meter of energy per electron added

% phicn = phig =4.5;% Carbon nanotube and gate metal work functions (eV)
% phis = phid = 4.63;% Source and Drain metal workfunctions (eV)

% Computation of the mid length self consistent field for a given Vgs
%----------------------------------------------------------------------
Vgs = 2; %Applied gate voltage (volt)
Vds = 0.2;%Drain voltage (volt)
U = 0; %Mid-length Self Consistent Field
dU = 1;%some initial value of error
while dU>1E-5
    charge = 0;
    for Energy = 0:0.01:1 %integrating from 0 to 0.5eV
        charge = charge + (D(Energy)*1.6E-19)*f(Energy-Vgs+U); %total charge pe
    end
    Unew = charge*Usingle; %potential energy for given charge density in eV
    dU = abs(U-Unew); %error in computation
    U = U + 0.01*(Unew-U);
```

```
end



% Computation and Plot of the Conduction and Valence Band Profiles for the
% applied Vds
% ------------------------------------------------------------------
CB = delta-(Vgs-U);% Mid length conduction band value
VB = CB - Eg;%Mid length Valence band value
index1 = 20; %dummy variable for array index
for i = 1:19
    length(i) = i-20;
    conduction_band_value(i) = 0;
    valence_band_value(i) = 0;
end
length(20)=-0.99;
for i = 0:0.1:6 %Running along length of tube from 0 to Rg
    index1 = index1 + 1;
    length(index1) = i;
    conduction_band_value(index1) = delta-(Vgs-U)*(i/6);
    valence_band_value(index1) = conduction_band_value(index1)-0.6;
end
for i = 1:88 %CB profile from Rg to (length of tube - Rg)
    length(index1+i) = 6+i;
```

```
    conduction_band_value(index1+i) = delta - (Vgs-U);
    valence_band_value(index1+i) = conduction_band_value(index1+i) - 0.6;
end
index1 = index1 + 88;
for i = 0:0.1:6 %Running along length of tube from Rg to drain end
    length(index1) = 6 + 88 + i;
    conduction_band_value(index1) = delta- Vds*i/6 - (Vgs-U)*(1-(i/6));
    valence_band_value(index1) = conduction_band_value(index1) - 0.6;
    index1 = index1 + 1;
end
for i = 0:20
    length(index1+i) = 6 + 88 + 6 + i;
    conduction_band_value(index1+i) = -Vds;
    valence_band_value(index1+i) = -Vds;
end

% hold on
% plot(length, conduction_band_value);
% plot(length, valence_band_value);
% grid on;
% hold off

%Computation of the VI characteristics by self consistent procedure
```

```
%-------------------------------------------------------------------
%This procedure involves calculating the barrier heights from the
%equilibrium Conduction band profile and then obtaining the transmission
%probabilities from them. Each of these probabilities is multiplied with
%the corresponding fermi function over the entire conduction band range
indexVds = 0
for Vds = 0:0.01:0.5
    indexVds = indexVds + 1;
    % Assume a quasi fermi level for electrons and holes: Reference electron qu
    % fermi level to source and hole quasi fermi level to drain
    Efn = 0;
    Efp = -Vds;
    % The Fermi function at Source contact is f(E) while within the nanotube it
    % shifts to f(E-Efn) and at the drain contact, it is f(E-q*Vds)

    %-------------------------------------------------
    % Self-consistent current calculation for electron
    %-------------------------------------------------
    dEf = 1;
    electron_count=0;% counter
    while abs(dEf) > 1E-5
        flux1= 0; flux2= 0; flux3= 0; flux4 = 0;
        for E = CB:0.01:delta
```

```
        %Source barrier height(hs) and width(ws) in nm
        hs = delta - E; ws = (Rg-Rt)*(delta-E)/(delta-CB);
        %Drain barrier height (hd) and width (wd) in nm
        hd = delta - Vds - E; wd = (Rg-Rt)*(delta-Vds-E)/(delta-Vds-CB);
        flux1 = flux1 + T(hs,ws)*f(E);
        flux2 = flux2 + T(hs,ws)*f(E-Efn);
        flux3 = flux3 + T(hd,wd)*f(E-Efn);
        flux4 = flux4 + T(hd,wd)*f(E+Vds);
    end
    dEf = (flux1-flux2)-(flux3-flux4);
    Efn = Efn + sign(dEf)*0.001;
    electron_count = electron_count + 1;
    if electron_count>500, break, end;
end

%Landauer formula for ballistic current. The addition q is to convert hbar
%to units of eV
electron_current(indexVds) = 2*(1.6E-19)^2/(pi*hbar) * (flux1-flux4);



%-----------------------------------------------
% Self-consistent current calculation for hole
%-----------------------------------------------
```

```
dEf = 1;
hole_count=0;% counter
while abs(dEf) > 1E-5
    flux5= 0; flux6= 0; flux7= 0; flux8 = 0;
    for E = abs(VB):0.01:1
        %Source barrier height(hs) and width(ws) in nm
        hs = delta - E; ws = (Rg-Rt)*(delta-E)/(delta-abs(VB));
        %Drain barrier height (hd) and width (wd) in nm
        hd = delta + Vds - E; wd = (Rg-Rt)*(delta+Vds-E)/(delta+Vds-abs(VB)
        flux5 = flux5 + T(hs,ws)*f(E);
        flux6 = flux6 + T(hs,ws)*f(E+Efp);
        flux7 = flux7 + T(hd,wd)*f(E+Efp);
        flux8 = flux8 + T(hd,wd)*f(E-Vds);
    end
    dEf = (flux8-flux7)-(flux6-flux5);
    Efp = Efp - sign(dEf)*0.001;
    hole_count = hole_count + 1;
    if hole_count>500, break, end;
end

%Landauer formula for ballistic current. The addition q is to convert hbar
%to units of eV
hole_current(indexVds) = 2*(1.6E-19)^2/(pi*hbar) * (flux8-flux7);
```

```
    Drain_current(indexVds) = electron_current(indexVds) + hole_current(indexVd
    drain_voltage(indexVds) = Vds;
end

hold on
plot(drain_voltage, Drain_current);
plot(drain_voltage, electron_current);
plot(drain_voltage, hole_current);
```